

EFFECT OF BEARING CHARACTERISTICS ON FREQUENCY RATIO OF ROTOR SYSTEM

B.B. Maharathi*

Abstract

Bearing characteristics play a major role for dynamical analysis of rotor-disk system. The dynamic characteristics include such as, critical speed, dynamic response, perfect balancing, threshold speed of instability and selection of optimum as well as stable bearings for rotor dynamics. This work highlights the comparison of stability characteristics of any rotor-disk model mounted on various kinds of hydrodynamic journal bearings with different length/diameter ratios. The bearings which are considered in this work are; the two-axial groove bearing, the four-axial groove bearing, the elliptical bearing, the two lobe bearing, the three-lobe bearing and the off-set cylindrical journal bearing with 0.5 and 1.0 as its length to diameter ratio. From the analysis is observed that the off-set cylindrical journal bearing is more stable than other bearings for any rotor model within the operating speed range. A three disks-rotor-bearing model mounted on different hydrodynamic journal bearings has been used for its dynamical analysis by using transfer matrix method based on continuous system model.

Nomenclature

[B] = bearing matrix
 C = radial clearance
 C_{zz}, C_{yy} = direct damping coefficient of bearing
 C_{zy}, C_{yz} = cross-coupled damping coefficient of the bearing
 D = diameter of the journal
 D_b = bearing diameter
 [D] = disk matrix
 e = eccentricity of the bearing
 $[\bar{F}]$ = overall field matrix
 K = non-dimensional parameter of the bearing
 K_{zz} = direct stiffness coefficients of the bearings
 K_{yy}
 K_{zy}, K_{yz} = cross-coupled stiffness coefficient of the bearings
 l = length of the rotor
 L_b = length of the bearing
 M = mass of the rotor at the bearing station
 M_t = effective mass of the rotor at the bearing
 N = revolution per minute
 R = radius of the journal
 S = Sommerfield number
 {S} = modified state vectors
 t = time
 W = radial load at bearing rotation

$[\bar{U}]$ = overall transfer matrix
 Y, Z = displacements of journal center in y and z directions, respectively
 ω = rotational speed, rad/s
 ω_a = critical speed of rigid rotor
 ρ = whirl frequency
 μ = viscosity of the lubricant
 λ = a number

Subscripts

O, n = stage numbers

Superscripts

- = refers to non-dimensional values

Introduction

Dynamic behaviour of rotor is commonly influenced by the bearing coefficients such as stiffness and damping. So the plain bearings are superior to rolling element bearings in high-speed operation. They have high damping ability, high load-carrying capacity and low friction. In addition, silent operation and long life can be attained. Therefore, plain bearings of various types are widely used in high-speed rotating machinery. The advantages are attributed to the mechanical characteristics of the thin

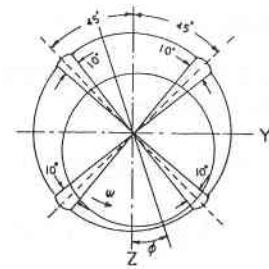
* Department of Mechanical Engineering, IGIT, Sarang-759 146, Orissa, India

Manuscript received on 20 Feb 2004; Paper reviewed, revised and accepted on Aug 2004

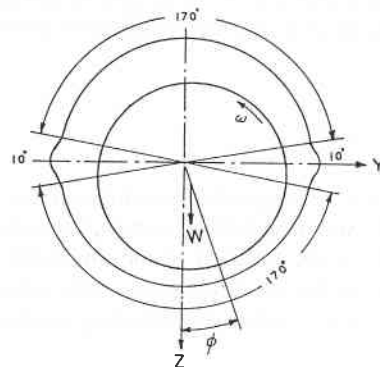
oil-film formed in the small clearance between journal and bearing surface. In many cases, the springs and damping characteristics of the lubricating oil-film have a most significant effect on the vibration of a shaft rotating in a journal bearing. Lund has made significant advancement in the field of rotor dynamics considering different aspects of fluid-film bearing characteristics [1-6]. Someya has given detail procedure for the evaluation of dynamic coefficients of hydrodynamic journal bearings [7]. Maharathi and Behera [8-16] have made significant advancement on dynamic analysis of rotor-bearing systems considering different critical parameter related rotor, disk and bearing.

In this work, an attempt has been made to determine for frequency ratio (v/ω) of a rotor system mounted on different hydrodynamic journal bearings with different (L/D) ratio shown in Fig.1 and they are as follows:

1. Two-axial groove bearing ($L/D = 0.5$ and 1.0)
2. Four-axial groove bearing ($L/D = 0.5$ and 1.0)
3. Elliptical bearing ($L/D = 0.5$ and 1.0)
4. Two-lobe bearing ($L/D = 0.5$ and 1.0)
5. Three-lobe bearing ($L/D =$ and 1.0)
6. Offset cylindrical bearing ($L/D = 0.5$ and 1.0).

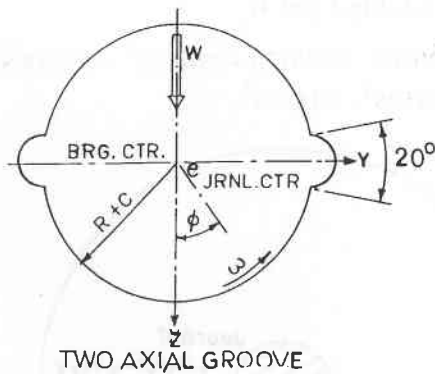


FOUR-AXIAL GROOVE

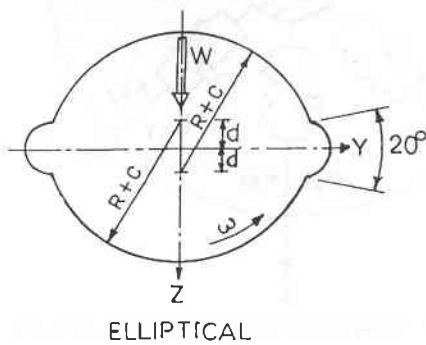


TWO-LOBE

Fig. 1b Different journal bearings

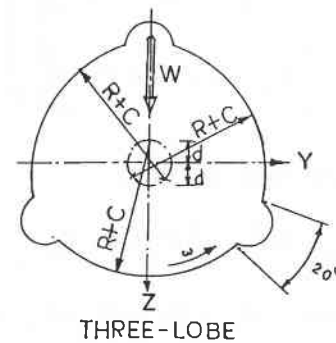


TWO AXIAL GROOVE

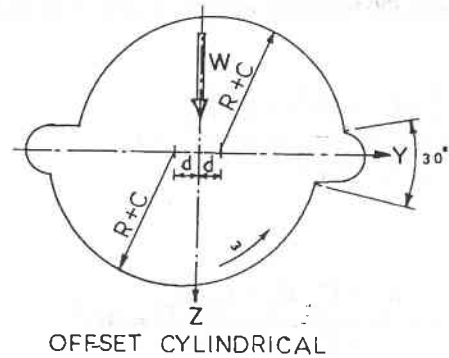


ELLIPTICAL

Fig. 1a Different journal bearings



THREE-LOBE



OFFSET CYLINDRICAL

Fig. 1c Different journal bearings

Theoretical Analysis

For a rigid rotor of mass $2M$, running in fluid-film bearings, the equations of motion are,

$$M \ddot{z} + K_{zz} z + K_{zy} y + C_{zz} \dot{z} + C_{zy} \dot{y} = 0 \tag{1a}$$

$$M \ddot{y} + K_{yy} y + K_{yz} z + C_{yy} \dot{y} + C_{yz} \dot{z} = 0 \tag{1b}$$

where 'M' is the mass per bearing. For a small disturbance from the equilibrium position of the journal, the vibrations of the journal is likely to occur in vertical and horizontal directions and their amplitudes of vibration are expressed as

$$z = Z e^{\lambda t}, y = Y e^{\lambda t} \tag{2}$$

where $\lambda = \alpha + i v$ is expressed in complex form. The real part posses the stability of the system and the complex part only is used for the solution of the threshold speed of instability 'v' is the whirl frequency of the rotor. Substituting Eq. (2) in (1), yields the following equation.

$$\begin{bmatrix} [(K_{zz} - M v^2) + i v C_{zz}] & (K_{zy} + i v C_{zy}) \\ (K_{zy} + i v C_{zy}) & [(K_{yy} - M v^2) + i v C_{yy}] \end{bmatrix} \begin{bmatrix} Z \\ Y \end{bmatrix} = 0 \tag{3}$$

For non-trivial values of Z and Y,

$$\begin{aligned} & (K_{zz} - M v^2) (K_{yy} - M v^2) - v^2 C_{zz} C_{yy} - K_{yz} K_{zy} \\ & + v^2 C_{zy} C_{yz} + i v [C_{zz} (K_{yy} - M v^2) + C_{yy} (K_{zz} - M v^2)] \\ & - i v (C_{yz} K_{zy} + K_{yz} C_{zy}) = 0 \end{aligned} \tag{4}$$

Separating the real and imaginary parts from Eq.(4), we have

$$\frac{(K_{zz} - M v^2) (K_{yy} - M v^2) - K_{zy} K_{zy}}{C_{zz} C_{yy} - C_{zy} C_{yz}} = v^2 \tag{5}$$

and

$$\frac{C_{zz} K_{yy} + C_{yy} K_{zz} - C_{yz} K_{zy} - C_{zy} K_{yz}}{C_{zz} + C_{yy}} = M v^2 \tag{6}$$

$$\text{Assuming } K = \frac{K_{zz} C_{yy} + C_{zz} K_{yy} - K_{zy} C_{yz} - C_{zy} K_{yz}}{C_{zz} + C_{yy}}$$

where K is an effective bearing stiffness and the critical mass at the bearing station will be

$$M_{crit} = \frac{K}{v^2} \tag{7}$$

Hence, the threshold speed of instability is determined by that speed at which the actual journal mass at the bearing station equals the critical mass. Therefore, the threshold speed of instability can be found out from the following equation:

$$\left(\frac{v}{\omega}\right)^2 = \frac{(K_{zz} - K) (K_{yy} - K) - K_{zy} K_{yz}}{\omega C_{zz} \omega C_{yy} - \omega C_{zy} \omega C_{yz}} \tag{8}$$

The linearised stiffness and damping coefficients of hydrodynamics journal bearings are shown in Fig.2 and are expressed in polynomial form in terms of the Sommerfeld number [17-19].

For Two-axial Groove Bearing
($L_b/D_b = 0.5$; Fig.3 and 4)

$$\begin{aligned} \bar{K}_{zz} = & 9.520766 - 25.2317S + 27.004S^2 - 12.2306S^3 \\ & + 2.3859S^4 - 0.1628S^5; \end{aligned}$$

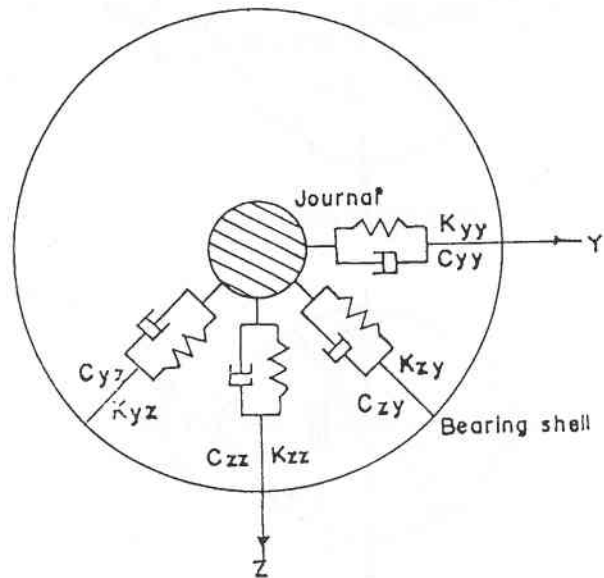


Fig. 2 Stiffness and damping characteristics of a journal bearing

$$\begin{aligned}
 \bar{K}_{zy} &= 4.8226 - 5.4034S + 7.041S^2 - 3.08186S^3 \\
 &\quad + 0.5946S^4 - 0.128S^5; \\
 \bar{K}_{yz} &= 0.801 - 4.1643S + 2.776S^2 - 1.094S^3 \\
 &\quad + 0.1956S^4 - 0.128S^5; \\
 \bar{K}_{yy} &= 1.5672 + 0.283S + 0.1253S^2 - 0.15237S^3 \\
 &\quad + 0.03924S^4 - 0.003S^5; \\
 \bar{C}_{zz} &= 8.7141 - 9.3046S + 12.7930S^2 - 5.6231S^3 \\
 &\quad + 1.0868S^4 - 0.0739S^5; \\
 \bar{C}_{zy} = \bar{C}_{yz} &= 1.7647 + 0.1939S + 0.3394S^2 - 0.3027S^3 \\
 &\quad + 0.075S^4 - 0.005S^5; \\
 \bar{C}_{yy} &= 0.7756 + 3.1191S - 0.3872S^2 - 0.10085S^3 \\
 &\quad + 0.0498S^4 - 0.0045S^5
 \end{aligned}
 \tag{9}$$

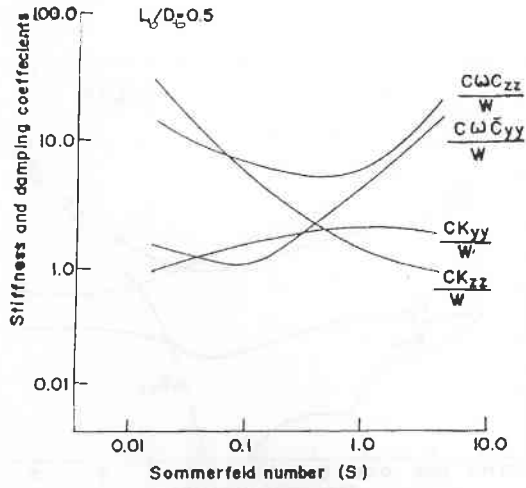


Fig. 3 Direct stiffness and damping coefficients of two-axial groove bearing ($L_b/D_b=0.5$)

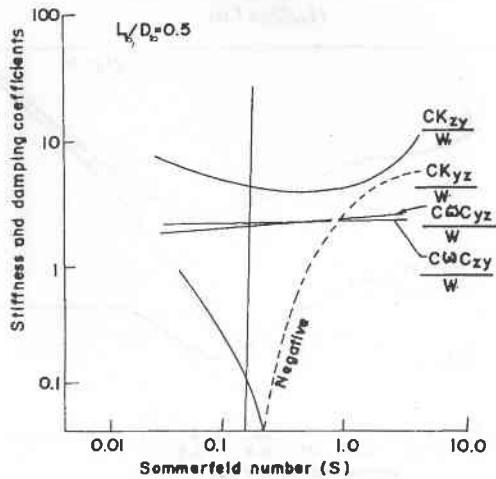


Fig. 4 Cross stiffness and damping coefficients of two-axial groove bearing ($L_b/D_b=0.5$)

For $L_b/D_b = 1.0$ (Figs.5 and 6)

$$\begin{aligned}
 \bar{K}_{zz} &= 10.5808 - 107.1318S + 459.1316S^2 - 841.8541S^3 \\
 &\quad + 670.3789S^4 - 189.3695S^5; \\
 \bar{K}_{zy} &= 4.818576 - 23.79633S + 115.3805S^2 - 204.55S^3 \\
 &\quad + 160.5203S^4 - 44.98935S^5; \\
 \bar{K}_{yz} &= 1.0812 - 18.29146S + 67.32996S^2 - 120.5438S^3 \\
 &\quad + 94.9635S^4 - 0.1135S^5; \\
 \bar{K}_{yy} &= 1.4561 + 0.1942S - 0.1135S^2; \\
 \bar{C}_{zz} &= 9.37864 - 39.8338S + 192.4017S^2 - 334.6719S^3 \\
 &\quad + 259.9724S^4 + 72.41817S^5; \\
 \bar{C}_{zy} = \bar{C}_{yz} &= 1.756928 - 0.15071S; \\
 \bar{C}_{yy} &= 0.55866 + 11.35037S - 31.9236S^2 + 56.0825S^3 \\
 &\quad - 43.9042S^4 + 12.347S^5
 \end{aligned}
 \tag{10}$$

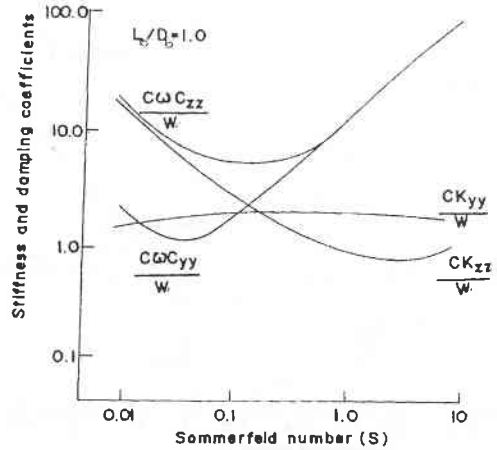


Fig. 5 Direct stiffness and damping coefficients of two-axial groove bearing ($L_b/D_b=1.0$)

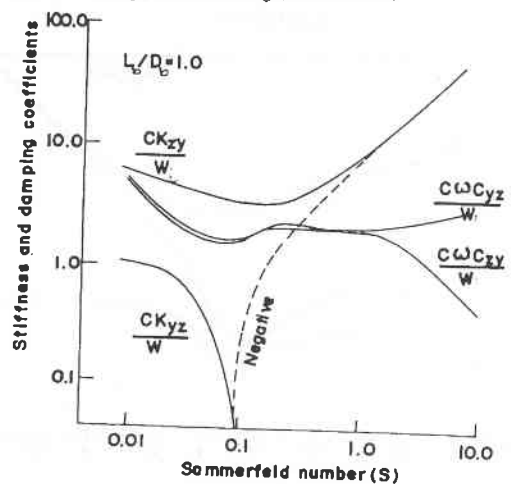


Fig. 6 Cross stiffness and damping coefficients of two-axial groove bearing ($L_b/D_b=1.0$)

**For Four-axial Groove Bearing
($L_b/D_b = 0.5$, Figs .7 and 8)**

$$\begin{aligned} \bar{K}_{zz} &= 15.1386 - 22.55S + 11.96S^2 - 2.587S^3 + 0.232S^4 \\ &\quad - 0.007S^5; \\ \bar{K}_{zy} &= 5.875 - 5.6423S + 3.1815S^2 - 0.638S^3 + 0.544S^4 \\ &\quad - 0.00157S^5; \\ \bar{K}_{yz} &= 0.8605 - 1.3461S + 0.009S^2; \\ \bar{K}_{yy} &= 1.2114 + 0.02258S; \\ \bar{C}_{zz} &= 11.3684 - 12.286S + 7.0836S^2 - 1.4506S^3 \\ &\quad + 0.1258S^4 - 0.0037S^5; \\ \bar{C}_{zy} &= 1.2534 + 0.0123S \\ \bar{K}_{yz} &= 1.2530 + 0.015263S \\ \bar{C}_{yy} &= 0.0975 + 2.1777S \end{aligned} \tag{11}$$

For $L_b/D_b = 1.0$ (Figs.9 and 10)

$$\begin{aligned} \bar{K}_{zz} &= 15.415 - 53.59S + 66.53S^2 - 32.295S^3 \\ &\quad + 6.176S^4 - 0.377S^5; \\ \bar{K}_{yy} &= 1.087 + 0.0215S \\ \bar{K}_{zy} &= 5.879 - 14.129S + 18.434S^2 - 8.56S^3 \\ &\quad + 1.6S^4 - 0.096S^5; \\ \bar{K}_{yz} &= 0.866 - 2.4608S + 0.035S^2; \\ \bar{C}_{zz} &= 11.984 - 32.349S + 42.5676S^2 - 11.944S^3 \\ &\quad + 3.746S^4 - 0.2265S^5; \\ \bar{C}_{yy} &= -0.0783 + 4.117S; \\ \bar{K}_{zy} &= 1.093 + 0.018S; \\ \bar{C}_{yz} &= 1.093 + 0.014S \end{aligned} \tag{12}$$

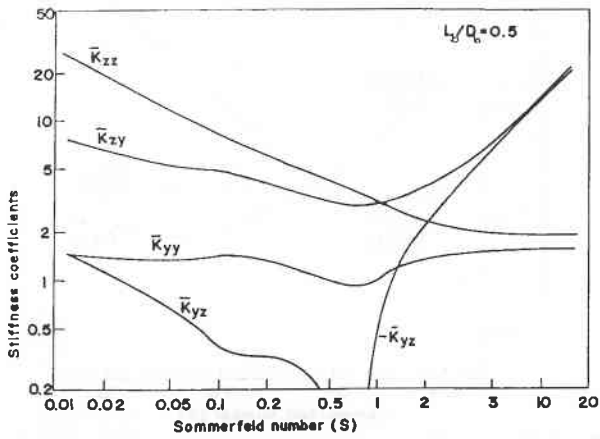


Fig. 7 Stiffness coefficients of four-axial groove bearing ($L_b/D_b=0.5$)

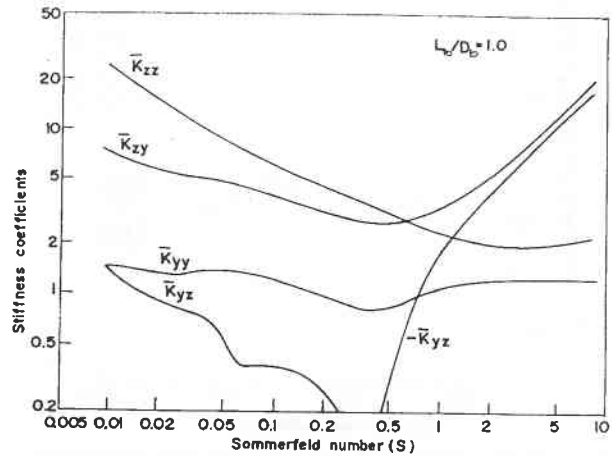


Fig. 9 Stiffness coefficients of four-axial groove bearing ($L_b/D_b=1.0$)

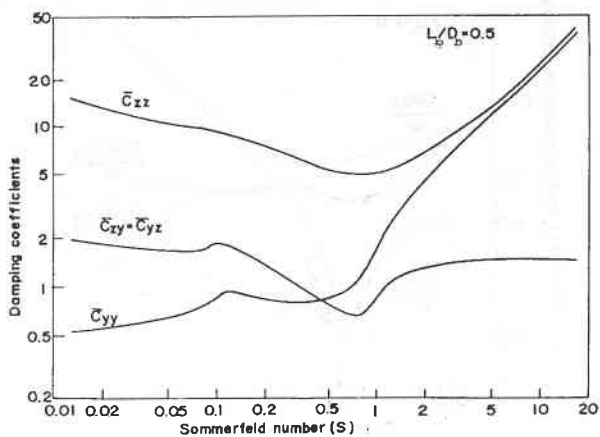


Fig. 8 Damping coefficients of four-axial groove bearing ($L_b/D_b=0.5$)

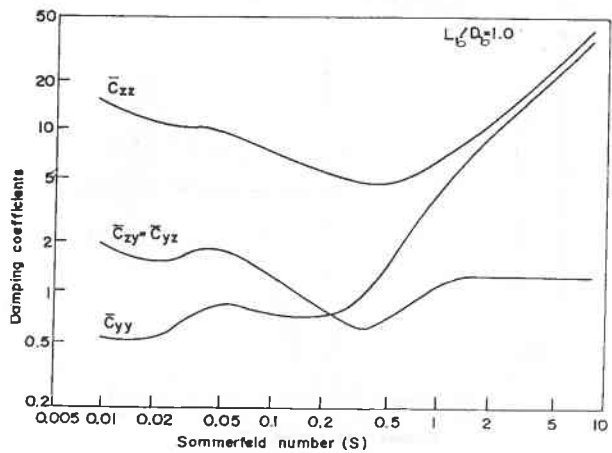


Fig. 10 Damping coefficients of four-axial groove bearing ($L_b/D_b=1.0$)

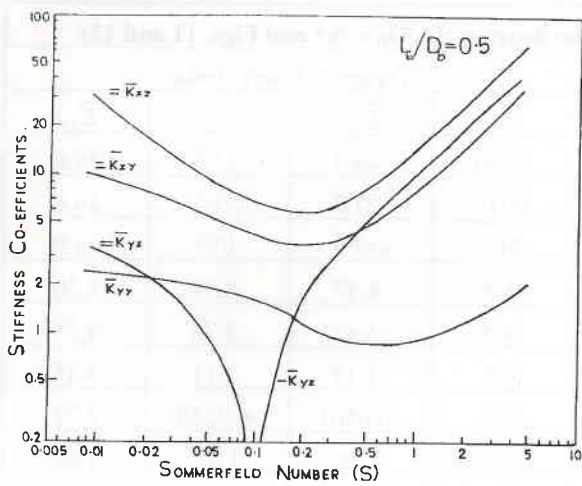


Fig. 11 Stiffness coefficients of two-lobe bearing ($L_b/D_b=0.5$)

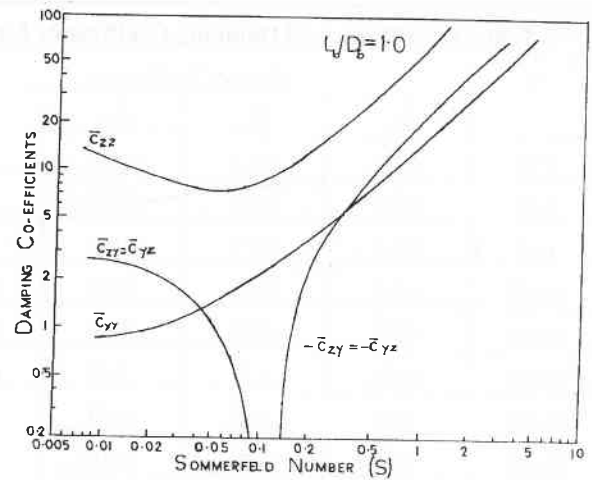


Fig. 14 Damping coefficients of two-lobe bearing ($L_b/D_b=1.0$)

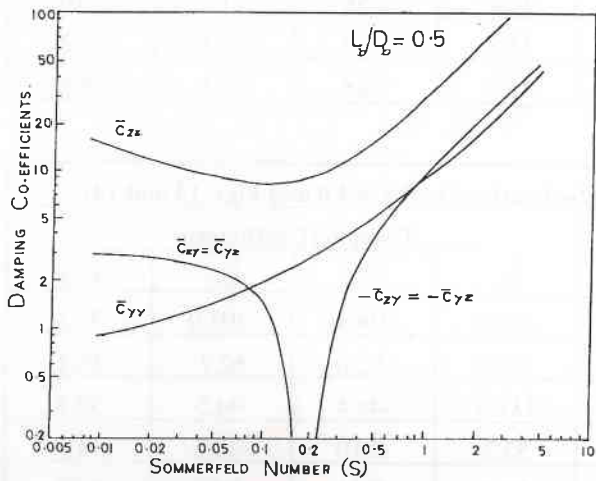


Fig. 12 Damping coefficients of two-lobe bearing ($L_b/D_b=0.5$)

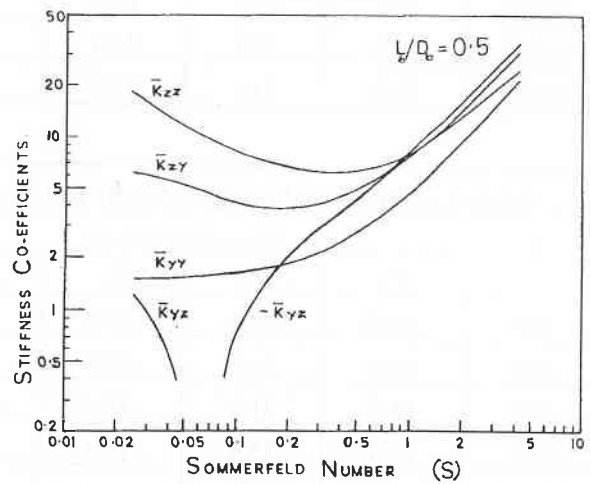


Fig. 15 Stiffness coefficients of three-lobe bearing ($L_b/D_b=0.5$)

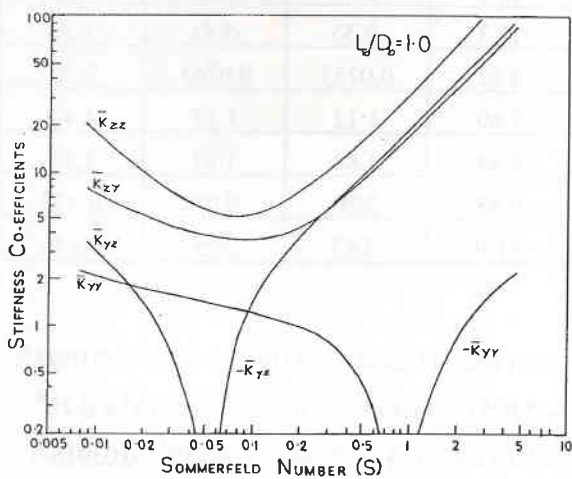


Fig. 13 Stiffness coefficients of two-lobe bearing ($L_b/D_b=1.0$)

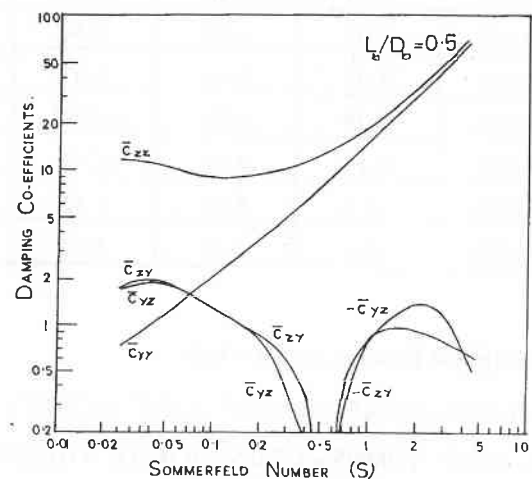


Fig. 16 Damping coefficients of three-lobe bearing ($L_b/D_b=0.5$)

S	Spring Coefficients				Damping Coefficients			
	\bar{K}_{zz}	\bar{K}_{zy}	\bar{K}_{yz}	\bar{K}_{yy}	\bar{C}_{zz}	\bar{C}_{zy}	\bar{C}_{yz}	\bar{C}_{yy}
4.79	61.5	33.1	-43.3	2.06	123.0	-43.3	-42.5	36.6
3.06	39.4	21.7	-28.0	1.43	80.0	-27.7	-27.7	23.4
1.93	25.1	13.7	-17.7	1.16	50.2	-17.9	-17.5	15.0
0.993	13.5	7.50	-9.20	0.897	26.5	-8.47	-8.34	8.20
0.496	7.88	4.52	-4.60	0.831	14.5	-3.42	-3.36	4.71
0.306	6.06	3.73	-2.82	0.940	10.5	-1.13	-1.11	3.45
0.209	5.66	3.60	-1.67	1.16	8.74	-0.0503	-0.0240	2.72
0.105	6.51	4.19	-0.015	1.57	7.86	1.44	1.45	1.89
0.0507	9.47	5.46	0.945	1.94	9.03	2.29	2.31	1.38
0.0303	13.2	6.45	1.72	2.12	10.4	2.58	2.62	1.16
0.0207	17.2	7.81	2.33	2.24	11.8	2.70	2.73	1.02
0.0100	29.6	9.68	3.28	2.39	15.3	2.88	2.93	0.875

S	Spring Coefficients				Damping Coefficients			
	\bar{K}_{zz}	\bar{K}_{zy}	\bar{K}_{yz}	\bar{K}_{yy}	\bar{C}_{zz}	\bar{C}_{zy}	\bar{C}_{yz}	\bar{C}_{yy}
4.99	140.0	7.74	-85.9	-2.15	282.0	-106.0	-107.0	73.3
2.93	82.7	45.1	-50.0	-1.34	167.0	-62.6	62.7	43.2
2.08	58.7	31.2	-35.4	-0.823	117.0	-44.4	-44.5	30.7
0.961	27.3	15.4	-16.4	-0.101	55.2	-20.0	-20.0	14.8
0.500	14.6	7.81	-8.61	0.424	28.0	-9.51	-9.59	8.00
0.305	9.53	5.36	-5.23	0.798	18.1	-5.10	-5.10	5.25
0.207	7.01	4.27	-3.59	0.977	13.3	-2.55	-5.51	3.28
0.104	5.03	3.40	-1.43	1.22	8.82	0.0753	0.0761	2.53
0.0496	5.78	3.78	0.0881	1.41	7.60	1.12	1.14	1.42
0.0291	8.13	4.51	0.775	1.60	8.44	1.84	1.87	1.11
0.0199	11.0	5.29	1.52	1.76	9.48	2.20	2.23	0.978
0.00993	19.1	7.42	3.20	2.09	11.9	2.63	2.65	0.856

For Elliptical Bearing ($L_b/D_b = 0.5$)

$$\bar{K}_{zz} = 6.2464 - 0.314S + 10.247S^2 - 2.95S^3 + 0.247S^4;$$

$$\bar{K}_{yy} = 1.6035 - 1.3602S + 0.738S^2 - 0.1631S^3 + 0.012S^4;$$

$$\bar{K}_{zy} = 4.076 - 1.602S + 5.18S^2 - 1.429S^3 + 0.1124S^4;$$

$$\bar{K}_{yz} = 1.1202 - 11.242S + 2.510S^2 - 0.716S^3 + 0.059S^4;$$

$$\bar{C}_{zz} = 5.9753 + 11.491S - 8.046S^2 - 2.2654S^3 + 0.2S^4$$

$$\bar{C}_{yy} = 0.691 + 7.72S - 1.524S^2 - 0.4643S^3 - 0.0391S^4;$$

$$\bar{C}_{zy} = 2.72 - 11.452S + 1.064S^2 - 0.203S^3 + 0.0134S^4$$

(13)

**Table-3 : Stiffness and Damping Coefficients for Three-lobe Bearing
($L_b/D_b = 0.5$ and Figs. 15 and 16)**

S	Spring Coefficients				Damping Coefficients			
	\bar{K}_{zz}	\bar{K}_{zy}	\bar{K}_{yz}	\bar{K}_{yy}	\bar{C}_{zz}	\bar{C}_{zy}	\bar{C}_{yz}	\bar{C}_{yy}
4.70	24.8	31.6	-33.4	22.0	69.8	-0.572	-0.462	65.8
2.33	13.9	15.8	-17.5	10.1	36.0	-0.844	-1.36	31.9
1.115	8.44	7.84	-8.72	4.94	19.2	-0.852	-0.816	15.4
0.695	6.84	5.70	-5.76	2.30	14.3	-0.220	-0.364	9.26
0.475	6.28	4.56	-4.03	2.76	11.6	0.109	0.125	6.58
0.330	6.28	4.24	-3.16	2.04	10.4	0.608	0.212	4.22
0.233	6.29	3.92	-2.32	2.10	9.34	0.728	0.740	4.08
0.159	7.67	3.88	-1.49	1.88	8.70	0.954	0.982	2.96
0.100	8.76	4.18	-0.604	1.66	8.74	1.24	1.24	1.99
0.050	11.92	5.30	0.348	1.60	10.40	1.82	1.83	1.23
0.0267	17.92	6.10	1.20	1.50	11.20	1.64	1.66	0.690

**Table-4 : Stiffness and Damping Coefficients for Three-lobe Bearing for Bearing
($L_b/D_b = 1.0$)**

S	Spring Coefficients				Damping Coefficients			
	\bar{K}_{zz}	\bar{K}_{zy}	\bar{K}_{yz}	\bar{K}_{yy}	\bar{C}_{zz}	\bar{C}_{zy}	\bar{C}_{yz}	\bar{C}_{yy}
3.256	28.31	43.30	-43.46	25.25	94.58	-1.11	-1.11	88.33
1.818	16.21	24.39	-24.34	13.70	54.59	-0.98	-0.98	48.27
1.243	12.21	16.93	-16.72	9.18	38.75	-0.84	-0.84	32.37
0.796	8.82	11.26	-10.82	5.80	26.62	-0.61	-0.61	20.15
0.574	7.24	8.55	-7.96	4.24	20.73	-0.37	-0.37	14.27
0.353	5.91	6.07	-5.62	2.89	15.15	0.06	0.06	8.70
0.245	5.48	5.01	-3.60	2.76	12.59	0.43	0.43	6.16
0.181	5.41	4.49	-2.74	2.09	11.20	0.73	0.73	4.73
0.138	5.54	4.22	-2.12	1.92	10.39	0.98	0.98	3.51
0.108	5.83	4.10	-1.65	1.8	9.91	1.18	1.18	3.16
0.085	6.25	4.08	-1.26	1.71	9.64	1.35	1.35	2.67
0.068	6.82	4.13	-0.92	1.62	9.54	1.48	1.48	2.19
0.062	7.05	4.17	-0.79	1.59	9.54	1.52	1.52	2.16
0.054	7.56	4.25	-0.57	1.54	9.57	1.57	1.57	1.92
0.034	9.70	4.65	0.11	1.42	10.03	1.67	1.67	1.23

S	Spring Coefficients				Damping Coefficients			
	\bar{K}_{zz}	\bar{K}_{zy}	\bar{K}_{yz}	\bar{K}_{yy}	\bar{C}_{zz}	\bar{C}_{zy}	\bar{C}_{yz}	\bar{C}_{yy}
6.519	47.06	82.04	5.48	64.74	97.59	45.00	45.00	59.71
4.240	23.60	41.06	2.64	32.32	49.04	22.62	22.62	29.94
2.805	15.81	27.42	1.65	21.49	32.97	15.22	15.22	20.06
2.081	11.93	20.61	1.12	16.05	25.01	11.50	11.56	15.15
1.339	8.08	13.79	0.54	10.56	17.15	7.98	7.98	10.25
0.953	6.18	10.39	0.20	7.78	13.34	6.31	6.31	7.83
0.717	5.14	8.45	-0.05	6.15	11.29	5.43	5.43	6.51
0.555	4.63	7.20	-0.09	5.000	10.00	4.76	4.76	5.38
0.493	4.56	6.72	0.01	4.53	9.49	4.38	4.38	4.74
0.353	4.63	5.78	0.22	3.53	8.51	3.56	3.56	3.40
0.284	4.85	5.40	0.33	3.08	8.17	3.18	3.18	2.79
0.228	5.018	5.15	0.42	2.74	7.99	2.88	2.98	2.34
0.182	5.65	5.01	0.51	2.48	7.95	2.65	2.65	1.98
0.162	5.93	4.97	0.55	2.37	7.97	2.55	2.55	1.82
0.143	6.26	4.95	0.60	2.27	8.02	2.46	2.46	1.69
0.126	6.64	4.95	0.65	2.19	8.10	2.38	2.38	1.56

S	Spring Coefficients				Damping Coefficients			
	\bar{K}_{zz}	\bar{K}_{zy}	\bar{K}_{yz}	\bar{K}_{yy}	\bar{C}_{zz}	\bar{C}_{zy}	\bar{C}_{yz}	\bar{C}_{yy}
3.780	52.12	83.73	8.14	56.69	113.96	42.08	42.08	47.10
1.882	26.12	41.89	3.99	21.31	67.20	21.13	21.13	23.61
1.247	17.45	27.95	2.57	18.83	38.38	14.19	14.19	15.81
0.927	13.13	20.99	1.83	14.08	29.04	10.76	10.76	11.93
0.596	8.74	13.89	1.05	9.22	19.61	7.33	7.33	8.00
0.418	6.44	10.17	0.62	6.68	14.73	6.04	6.04	5.96
0.316	5.22	8.13	0.33	5.26	12.18	4.88	4.88	4.90
0.248	4.49	6.87	0.11	4.35	10.71	4.30	4.30	4.28
0.198	4.08	6.02	-0.04	3.70	9.80	3.99	3.99	3.83
0.160	4.00	5.40	0.01	3.17	9.07	3.57	3.57	3.22
0.130	4.13	4.96	0.12	2.76	8.55	3.15	3.15	2.65
0.107	4.37	4.68	0.22	2.46	8.23	2.64	2.64	2.22
0.087	4.74	4.50	0.31	2.23	8.08	2.60	2.60	1.89
0.078	4.98	4.45	0.36	2.14	8.06	2.50	2.50	1.75
0.070	5.25	4.42	0.41	2.00	8.07	2.42	2.42	1.62

For $L_b/D_b = 1.0$

$$\begin{aligned} \bar{K}_{zz} &= 6.772 - 37.1125S - 110.99S^2 - 454.752S^3 \\ &\quad + 373.570S^4 - 110.387S^5; \\ \bar{K}_{yy} &= 1.557 - 3.7202S + 2.0452S^2 - 0.579S^3; \\ \bar{C}_{zy} &= 4.0577 - 13.1145S + 96.256S^2 - 155.533S^3 \\ &\quad + 116.4065S^4 - 32.014S^5; \\ \bar{K}_{yz} &= 1.3276 - 26.9315S + 33.747S^2 - 41.655S^3 \\ &\quad + 20.722S^4 - 3.128S^5; \\ \bar{C}_{zz} &= 7.1394 - 3.06S + 211.5S^2 - 365.474S^3 + \\ &\quad 289.474S^4 - 83.404S^5; \\ \bar{C}_{yy} &= 0.2606 + 21.7633S - 35.5711S + 51.787S^3 \\ &\quad - 31.183S^4 + 6.490S^5; \\ \bar{C}_{yy} &= 0.2606 + 21.7633S - 35.5711S + 51.787S^3 \\ &\quad - 31.183S^4 + 6.490S^5; \\ \bar{C}_{zy} &= \bar{C}_{yz} = 2.6032 - 19.7309S - 26.2215S^2 + 68.1665S^3 \\ &\quad - 66.6116S^4 + 21.7890S^5 \end{aligned} \tag{14}$$

where

$$\begin{aligned} S &= \frac{\mu DLN}{60 \times W} \times (R/C)^2; \bar{K}_{zz} = \frac{CK_{zz}}{W}; \bar{K}_{yy} = \frac{CK_{yy}}{W}; \\ \bar{K}_{zy} &= \frac{CK_{zy}}{W}; \bar{K}_{yz} = \frac{CK_{yz}}{W}; \bar{C}_{zz} = \frac{C \omega C_{zz}}{W}; \bar{C}_{yy} = \frac{C \omega C_{yy}}{W}; \\ \bar{C}_{zy} &= \frac{C \omega C_{zy}}{W}; \bar{C}_{yz} = \frac{C \omega C_{yz}}{W} \end{aligned} \tag{14}$$

A simple Jeffcott rotor as shown in Fig.17 is considered in the present analysis to find out the (ν/ω) ratio of the model mounted on different hydrodynamic journal bearings.

- Total Mass of the model = 453.6 kg
- Mass at each bearing station (M) = 226.8 kg
- Radial clearance (C) = 0.00508×10^{-2} m
- Journal diameter (D_b) = 10.16×10^{-2} m
- Oil-viscosity (μ) = 5.68×10^{-3} N-s/m²

$$\omega = \frac{2 \pi N}{60} \text{ rad/sec, } L_b/D_b = 0.5 \text{ and } 1.0$$

The Sommerfeld number is first determined at each operating speed and the bearing coefficient are evaluated to obtain the effective bearing stiffness. Than the ratio of whirl frequency (ν) and rotational speed (ω) is determined to suggest the suitable bearing. The results of this analysis is presented in Table-7.

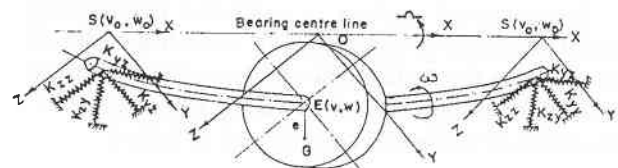


Fig. 17 A simple Jeffcott rotor model

Table-7 : Comparison of Frequency Ratio of Rotor Mounted on Different Journal Bearings

Name of the bearing	$\frac{\text{Length}}{\text{Diameter}} = \frac{L_b}{D_b}$	$\frac{\text{whirl frequency}}{\text{rotational frequency}} = \frac{\nu}{\omega}$
Two-Axial Groove	0.5	0.412
	1.0	0.435
Four-Axial Groove	0.5	0.438
	1.0	0.457
Elliptical	0.5	0.473
	1.0	0.487
Two-lobe	0.5	0.485
	1.0	0.488
Three-lobe	0.5	0.487
	1.0	0.489
Off-set Cylindrical	0.5	0.326
	1.0	0.338

Significance of Bearing Characteristics

A rotating system consisting of rotor, rigid disks and linear flexible bearings as shown in Fig.18 is considered in the present analysis. The system transfer matrix is obtained by utilizing the field and point transfer matrices to sequentially transfer the rotor state from left boundary point-n [20]. This sequential application gives :

$$\{\bar{S}\}_n^R = [\bar{U}] \{\bar{S}\}_0^L \tag{15}$$

where

$$[\bar{U}] = [\bar{F}]_n [B] [\bar{F}]_{n-1} \dots [D] [\bar{F}]_4 [D] [\bar{F}]_3 [D] [\bar{F}]_2 [B] [\bar{F}]_1$$

Since the shear force and bending moments are zero at both ends, a set of eight linear equations can be solved to determine the state variables at the starting station denoted by $\{\bar{S}\}_0^L$. Then the state vectors at every station can be obtained to get the dynamic response of a rotor system.

Numerical Analysis

For numerical analysis, a simplified rotor-bearing model consisting of three-disks of equal mass with an unbalance in the middle disk and two plain cylindrical bearings for its supports as shown in Fig.19 has been used. The details of this model are presented in Table-8.

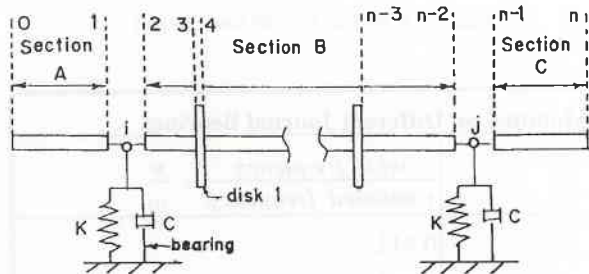


Fig. 18 A general rotor-bearing system

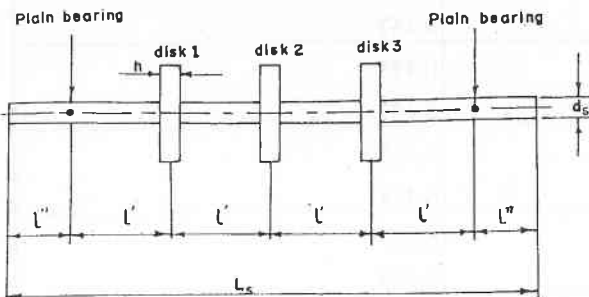


Fig. 19 A three disk-rotor-bearing model for numerical analysis ($d_s=0.04m$, $h=0.04m$, $L_s=1.062m$, $l'=0.2m$ and $l''=0.131m$)

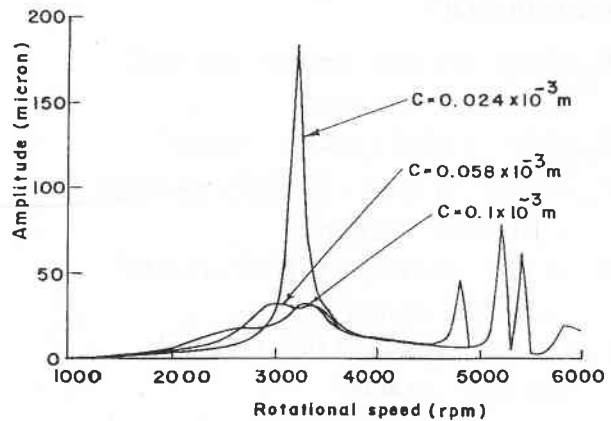


Fig. 20 Variation of dynamic response of rotor with clearance ($\mu=17 \times 10^{-3}Ns/m^2$, $D_b=40.396 \times 10^{-3}m$, plain cylindrical bearing, $L_b/D_b=0.5$)

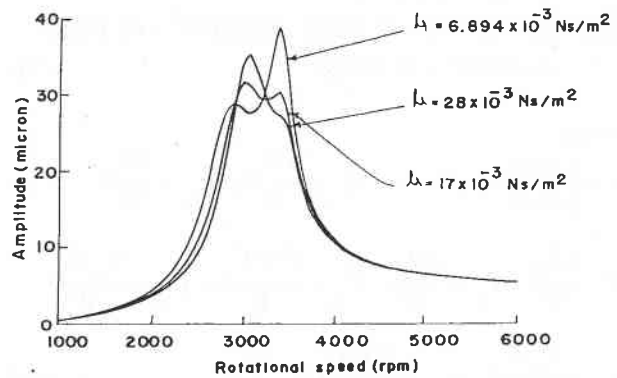


Fig. 21 Variation of dynamic response of rotor with viscosity ($C=0.058 \times 10^{-3}m$, $D_b=40.116 \times 10^{-3}m$, plain cylindrical bearing, $L_b/D_b=0.5$)

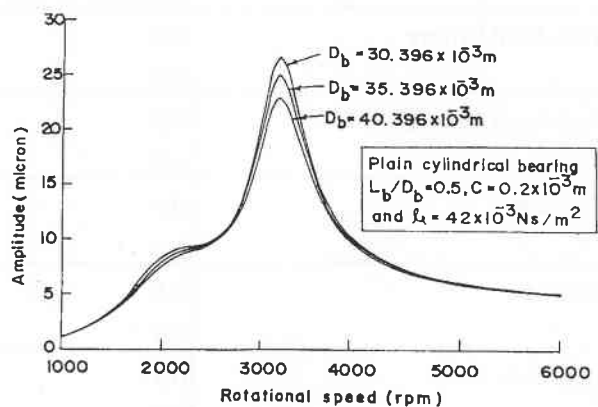


Fig. 22 Variation of dynamic response of rotor with bearing diameter ($C=0.2 \times 10^{-3}m$, $\mu=42 \times 10^{-3}Ns/m^2$, plain cylindrical bearing, $L_b/D_b=0.5$)

The dynamic response of this model at the middle disk mounted at different journal bearings has been evaluated by the transfer matrix method [20]. The variation of dynamic response due to bearing parameters (bearing diameter, oil viscosity and bearing clearance) are shown in Figs. 20-33. Further, a set of comparison has been made on dynamic response between the initial and optimal values of the bearing parameters [20] and the numerical results are also presented in Figs.34-41 and in Table-9.

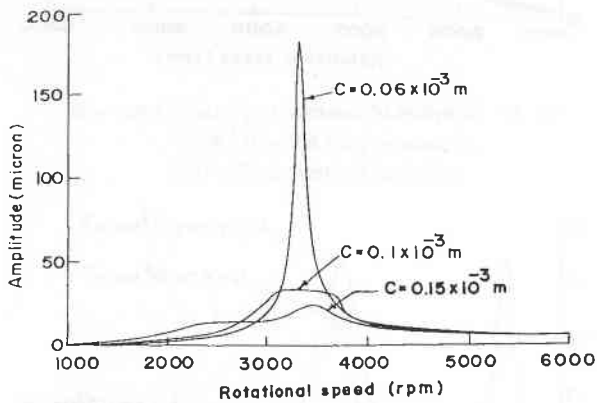


Fig. 23 Variation of dynamic response of rotor with clearance ($\mu=28 \times 10^{-3} \text{Ns/m}^2$, $D_b=40.396 \times 10^{-3} \text{m}$, plain cylindrical bearing, $L_b/D_b=1.0$)

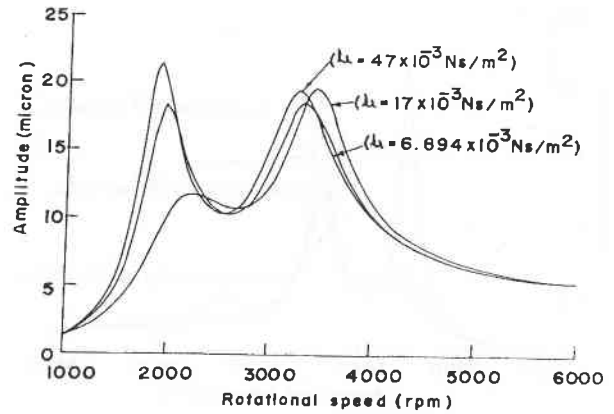


Fig. 24 Variation of dynamic response of rotor with viscosity ($C=0.2 \times 10^{-3} \text{m}$, $D_b=40.396 \times 10^{-3} \text{m}$, plain cylindrical bearing, $L_b/D_b=1.0$)

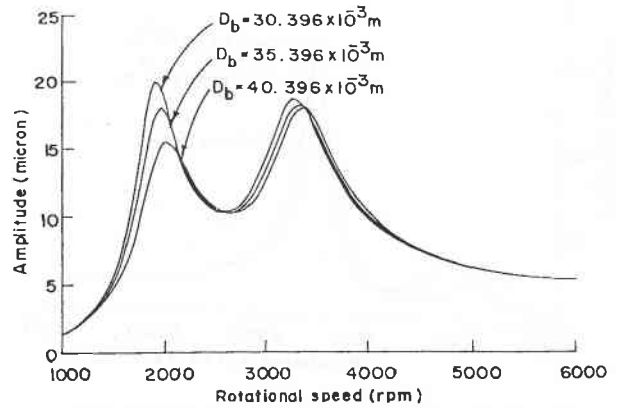


Fig. 25 Variation of dynamic response of rotor with bearing diameter D_b ($C=0.2 \times 10^{-3} \text{m}$, $\mu=42 \times 10^{-3} \text{Ns/m}^2$, plain cylindrical bearing, $L_b/D_b=1.0$)

Table-8 : The Details of Three-Disk Rotor System	
Details of Shaft	
i) Young's modulus (E)	$2.07 \times 10^{11} \text{N/m}^2$
ii) Shear modulus (G)	$8.10 \times 10^{10} \text{N/m}^2$
iii) Shape factor (α)	0.75
iv) Mass density (ρ)	$7.75 \times 10^3 \text{kg/m}^3$
Details of Disks	
i) Mass of each disk (M_d)	13.47 kg
ii) Diameter of each disk (D)	0.24 m
iii) Thickness of each disk (h)	0.04 m
iv) Unbalance at the middle disk	$120 \times 10^{-6} \text{kg-m}$
Details of Bearings	
i) Length (L_b)	$2.40 \times 10^{-2} \text{m}$
ii) Diameter (D_b)	$40.396 \times 10^{-3} \text{m}$
iii) Clearance (C)	$0.20 \times 10^{-3} \text{m}$
Viscosity (μ)	$47.00 \times 10^{-3} \text{Ns/m}^2$

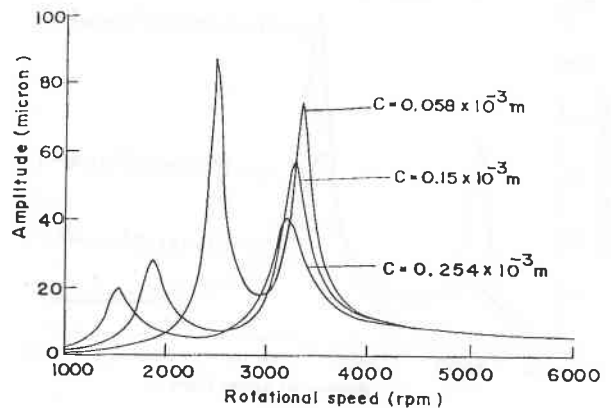


Fig. 26 Variation of dynamic response of rotor with clearance ($\mu=6.894 \times 10^{-3} \text{Ns/m}^2$, four axial grooved bearing, $L_b/D_b=0.5$)

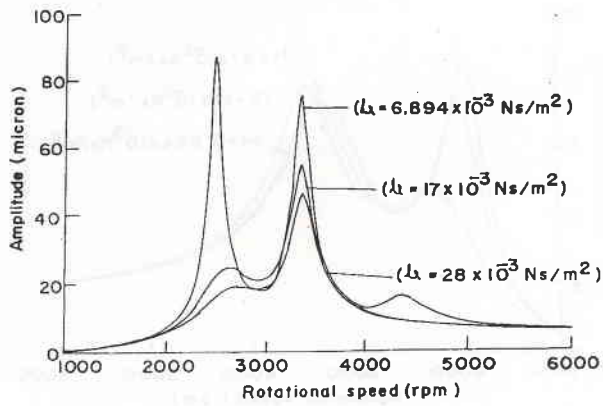


Fig. 27 Variation of dynamic response of rotor with viscosity ($C=0.058 \times 10^{-3} \text{ m}$, four axial grooved bearing, $L_b/D_b=1.0$)

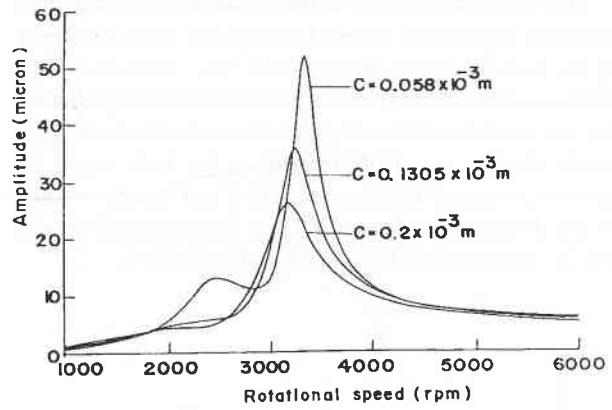


Fig. 30 Variation of dynamic response of rotor with clearance ($\mu=1.639 \times 10^{-3} \text{ Ns/m}^2$, elliptical bearing, $L_b/D_b=0.5$)

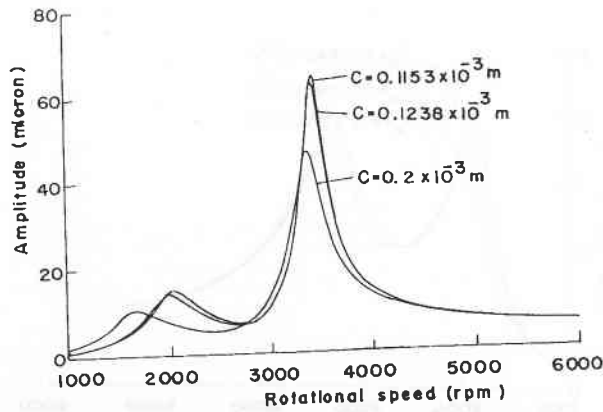


Fig. 28 Variation of dynamic response of rotor with clearance ($\mu=1.683 \times 10^{-3} \text{ Ns/m}^2$, four axial grooved bearing, $L_b/D_b=1.0$)

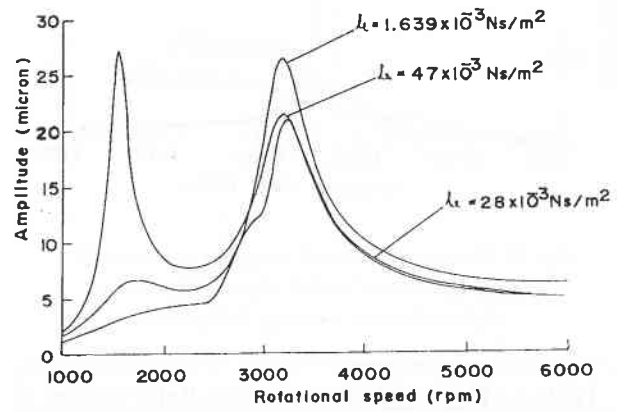


Fig. 31 Variation of dynamic response of rotor with viscosity ($C=0.2 \times 10^{-3} \text{ m}$, elliptical bearing, $L_b/D_b=0.5$)

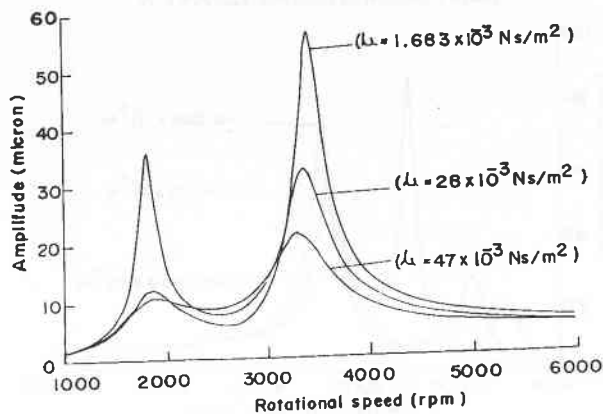


Fig. 29 Variation of dynamic response of rotor with viscosity ($C=0.15 \times 10^{-3} \text{ m}$, four axial grooved bearing, $L_b/D_b=1.0$)

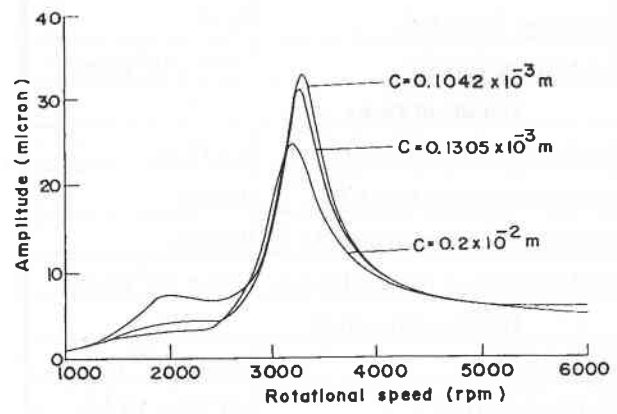


Fig. 32 Variation of dynamic response of rotor with clearance ($\mu=2.758 \times 10^{-3} \text{ Ns/m}^2$, elliptical bearing, $L_b/D_b=1.0$)

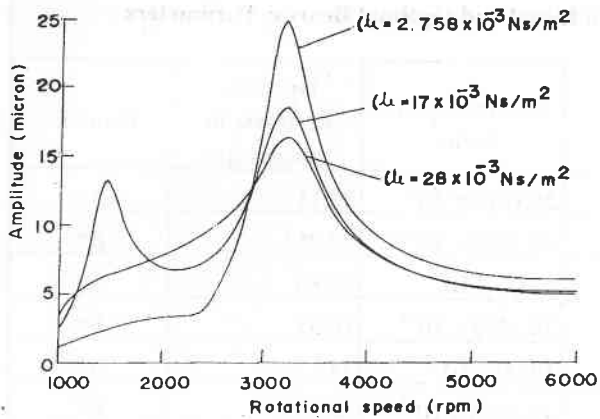


Fig. 33 Variation of dynamic response of rotor with viscosity ($C=0.2 \times 10^{-3}$ m, elliptical bearing, $L_b/D_b=1.0$)

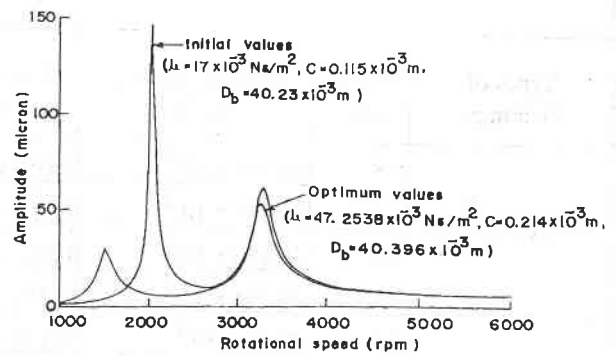


Fig. 36 Variation of dynamic response of rotor with and without optimum bearing parameters (Four axial grooved bearing, $L_b/D_b=0.5$)

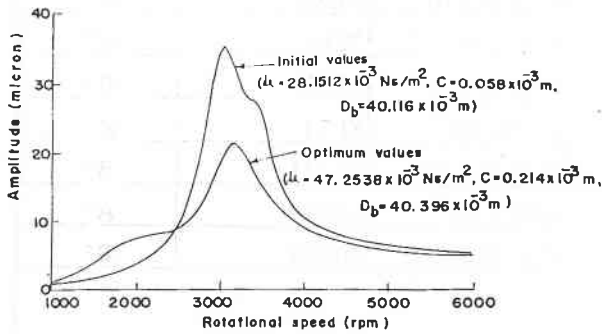


Fig. 34 Variation of dynamic response of rotor with and without optimum bearing parameters (Plain cylindrical bearing, $L_b/D_b=0.5$)

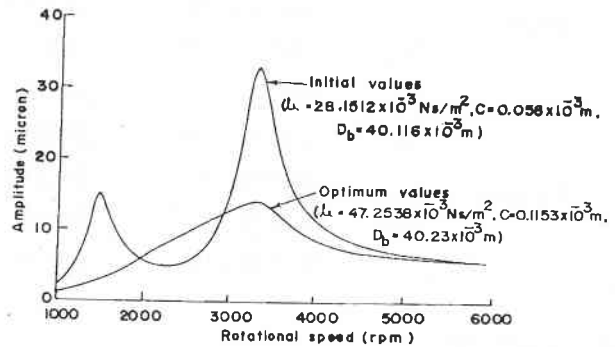


Fig. 37 Variation of dynamic response of rotor with and without optimum bearing parameters (Four axial grooved bearing, $L_b/D_b=1.0$)

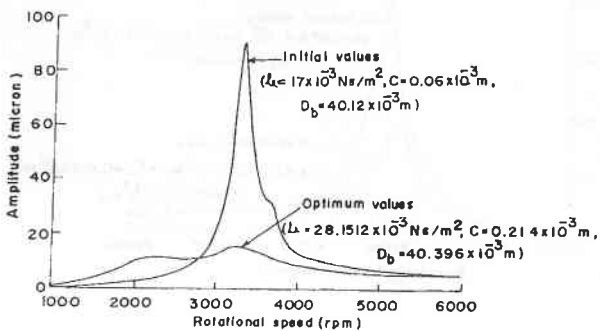


Fig. 35 Variation of dynamic response of rotor with and without optimum bearing parameters (Plain cylindrical bearing, $L_b/D_b=1.0$)

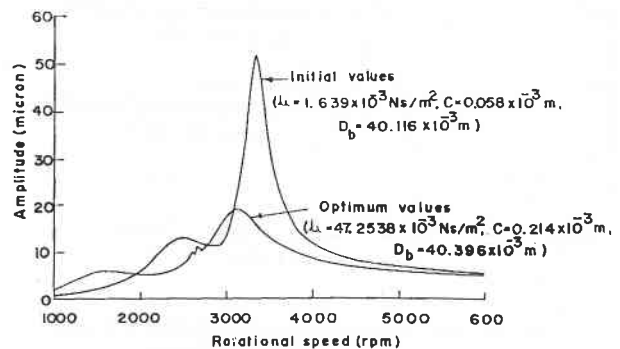


Fig. 38 Variation of dynamic response of rotor with and without optimum bearing parameters (Elliptical bearing, $L_b/D_b=0.5$)

Table-9 : Comparison of Dynamic Response Between Initial and Optimal Bearing Parameters

Types of Bearings	L_b/D_b ratio	Bearing Diameter (D_b) in m	Clearance (C) in m	Viscosity (μ) in Ns/m^2	Dynamic Response in micron (μ)	Remarks
Plain cylindrical	0.5	40.116×10^{-3}	0.058×10^{-3}	28.1512×10^{-3}	35.11	A*
		40.396×10^{-3}	0.214×10^{-3}	47.2538×10^{-3}	20.952	B*
	1.0	40.120×10^{-3}	0.06×10^{-3}	17.00×10^{-3}	90.80	A*
		40.396×10^{-3}	0.214×10^{-3}	28.1512×10^{-3}	16.55	B*
Four axial grooved	0.5	40.23×10^{-3}	0.115×10^{-3}	17.00×10^{-3}	149.33	A*
		40.396×10^{-3}	0.214×10^{-3}	47.2538×10^{-3}	38.453	B*
	1.0	40.116×10^{-3}	0.058×10^{-3}	28.1512×10^{-3}	32.95	A*
		40.2306×10^{-3}	0.1153×10^{-3}	47.2538×10^{-3}	13.98	B*
Elliptical	0.5	40.116×10^{-3}	0.058×10^{-3}	1.639×10^{-3}	52.64	A*
		40.396×10^{-3}	0.214×10^{-3}	47.2538×10^{-3}	19.089	B*
	1.5	40.2037×10^{-3}	0.1016×10^{-3}	2.758×10^{-3}	32.81	A*
		40.396×10^{-3}	0.214×10^{-3}	47.2538×10^{-3}	13.559	B*
Five pad	0.5	40.2032×10^{-3}	0.1016×10^{-3}	1.379×10^{-3}	81.74	A*
		40.396×10^{-3}	0.214×10^{-3}	47.2538×10^{-3}	35.334	B*
	1.0	40.116×10^{-3}	0.058×10^{-3}	3.447×10^{-3}	64.04	A*
		40.396×10^{-3}	0.2032×10^{-3}	42.1974×10^{-3}	20.908	B*

A* : Initial values
 B* : Optimum values

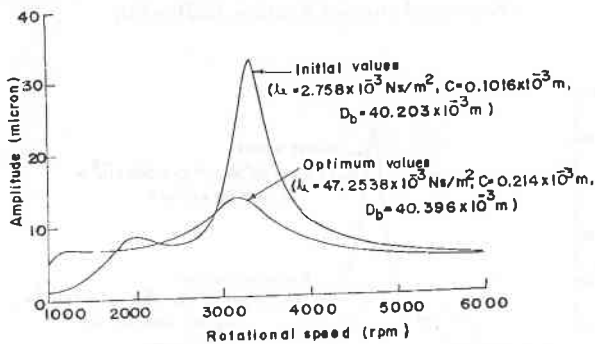


Fig. 39 Variation of dynamic response of rotor with and without optimum bearing parameters (Elliptical bearing, $L_b/D_b=1.0$)

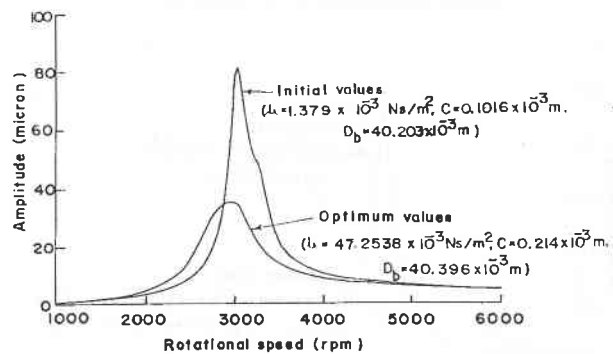


Fig. 40 Variation of dynamic response of rotor with and without optimum bearing parameters (Five-pad bearing, $L_b/D_b=0.5$)

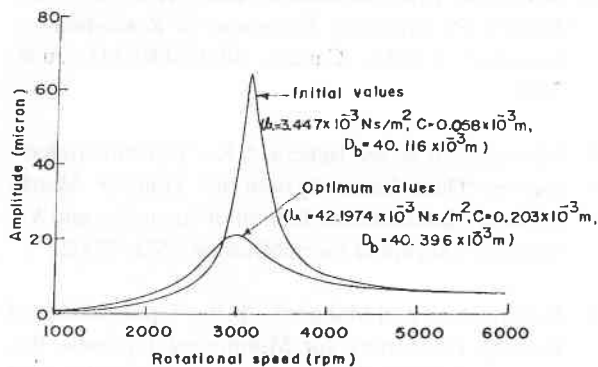


Fig. 41 Variation of dynamic response of rotor with and without optimum bearing parameters (Five-pad bearing, $L_b/D_b=1.0$)

Conclusions

1. The threshold speed of instability is the speed at which critical mass (M_c) is equal to the mass (M) at bearing station.
2. Generally, the oil-whirl takes place for the frequency ratio of 0.4-0.5 for most of the speed. From the numerical results, it is observed that the frequency ratio of all the bearings lies between 0.4 to 0.5 except the off-set cylindrical bearings.
3. Since the frequency ratio (v/ω) of the off-set cylindrical bearing is much lower than 0.4, so that this bearing type is expected to be more stable for any rotor system within its operating speed range.
4. The physical bearing parameters significantly alter the dynamic response of the rotor system because the dynamic characteristics of rotor-bearing systems are greatly influenced by the bearing coefficients.
5. The maximum dynamic response of the rotor can be minimized by choosing the most optimum bearing parameters.

Acknowledgement

The work has been carried out under the grant of AICTE Project (F.No./8020RIP/R&D) 75.2001-02), Government of India.

References

1. Lund, J.W., "Rotor bearings Dynamic Technology, Part III", Design Handbook for Fluid Film Bearings, Mechanical Technology Inc., AFAPL-Tr-65-45, 1965.
2. Lund, J.W. and Orcutt, F.K., "Calculations and Experiments on the Unbalance Response of a Flexible Rotor", Journal of Engineering for Industry, Trans of ASME, Vol.89, pp.785-796, 1967.
3. Lund, J.W., "Stability and Damped Critical Speeds of a Flexible Rotor in Fluid-Film Bearings", Journal of Engineering for Industry, Trans. Of ASME, Vol.96, pp.509-517, 1974.
4. Lund, J.W., "Modal Response of a Flexible Rotor in Fluid-Film Bearing", Journal of Engineering for Industry, Trans. of ASME, Vol.96, pp.525-533, 1974.
5. Lund, J.W., "A Calculation Method and Data for the Dynamic Coefficients of Oil Lubricated Journal Bearings", The Design Engineering Conference, Chicago, Illinois, USA, pp.1-28, April, 1978.
6. Someya, T., Journal-Bearing Data Book, Springer-Verlag, Berlin, 1988.
7. Prabhu, B.S., "An Experimental Investigation on the Misalignment Effects in Journal Bearings", Tribology Transactions, Vol.40, No.2, pp.235-242, 1997.
8. Maharathi, B.B. and Behera, A.K., "Dynamic Behaviour Analysis of Rotor-Bearing Systems by an Improved Transfer Matrix Method", Journal of Aeronautical Society of India, Vol.51, No.2, pp.72-82, 1999.
9. Maharathi, B.B. and Behera, A.K., "Parametric Study on Dynamic Behaviour of Rotor-Bearing Systems", Journal of Aeronautical Society of India, Vol.51, No.3, pp.152-162, 1999.
10. Maharathi, B.B. and Behera, A.K., "A Transfer Matrix Method for Dynamic Behaviour of Rotor-Bearing Systems", Journal of Aeronautical Society of India, Vol.51, No.4, pp.214-224, 1999.
11. Maharathi, B.B. and Behera, A.K., "Comparative Study of Unbalance Response and Critical Speeds of Rotor-Bearing Systems", Journal of the Institution of Engineers (India), Vol.80, pp.95-100, 1999.
12. Maharathi, B.B. and Behera, A.K., "Effect of Disk Flexibility on Rotor Dynamics", Journal of Aeronautical Society of India, Vol.52, No.1, pp.9-18, 2000.

13. Maharathi, B.B. and Behera, A.K., "Dynamic Behaviour Analysis of Continuous Rotor System", Journal of Structural Engineering (CSIR), India, Vol.28, No.2, pp.81-88, 2001.
14. Maharathi, B.B., Das, P.R. and Behera, A.K., "Dynamic Behaviour Analysis of Bowed Rotor by Transfer Matrix Method", Journal of Aeronautical Society of India, Vol.53, No.4, pp.217-225, 2001.
15. Maharathi, B.B. and Behera, A.K., "Dynamic Analysis of Turbine Rotors by Distributed Elements", Journal of the Institution of Engineers (India), Vol.82, pp.63-68, 2001.
16. Maharathi, B.B. and Behera, A.K., "Transfer Matrix Analysis of High Speed Rotors by Distributed Elements", Transactions of Mechanical Engineering, Australia, Vol.ME25, No.1, pp.21-30, 2001.
17. Maharathi, B.B. and Behera, A.K., "Transfer Matrix Method for Dynamic Behaviour of Rotor-Bearing Systems", CSME, Canada (99-CSME-11), June, 2001.
18. Maharathi, B.B. and Behera, A.K., "Dynamic Behaviour of Dual Rotor System by Transfer Matrix Method", International Journal of Acoustics and Vibrations (Accepted for publication), May 2002.
19. Behera, A.K. and Maharathi, B.B., "Optimization of Bearing Parameters for Minimising Dynamic Response of Rotor-Bearing System", Proceedings of Seventh International Congress on Sound and Vibration, Germany, pp.787-794, July 4-7, 2000.
20. Maharathi, B.B., "Study on Dynamics of Rotor Bearing Systems and Optimization of Rotor Bearing Parameters for Minimum Rotor Unbalance Response", Ph.D. Dissertation, Sambalpur University, REC, Rourkela, 2003.